Electronic Supporting Information

High *n*-caprylate productivities and specificities with dilute ethanol and acetate: chain elongation with microbiomes to upgrade products from syngas fermentation

Leo A. Kucek[a], Catherine M. Spirito[a], and Largus T. Angenent[a,b]*

[a]Department of Biological and Environmental Engineering, Cornell University, Riley-Robb Hall, Ithaca, NY 14853, USA.

[b]Center for Applied Geosciences, University of Tübingen, Hölderlinstr. 12, 72074 Tübingen, Germany.

* Corresponding author: Center for Applied Geosciences, University of Tübingen, Hölderlinstr. 12, 72074 Tübingen │ GermanyPhone: +49-07071-601322 │ Fax: +49-07071-6011308 │ E-mail: l.angenent@uni-tuebingen.de

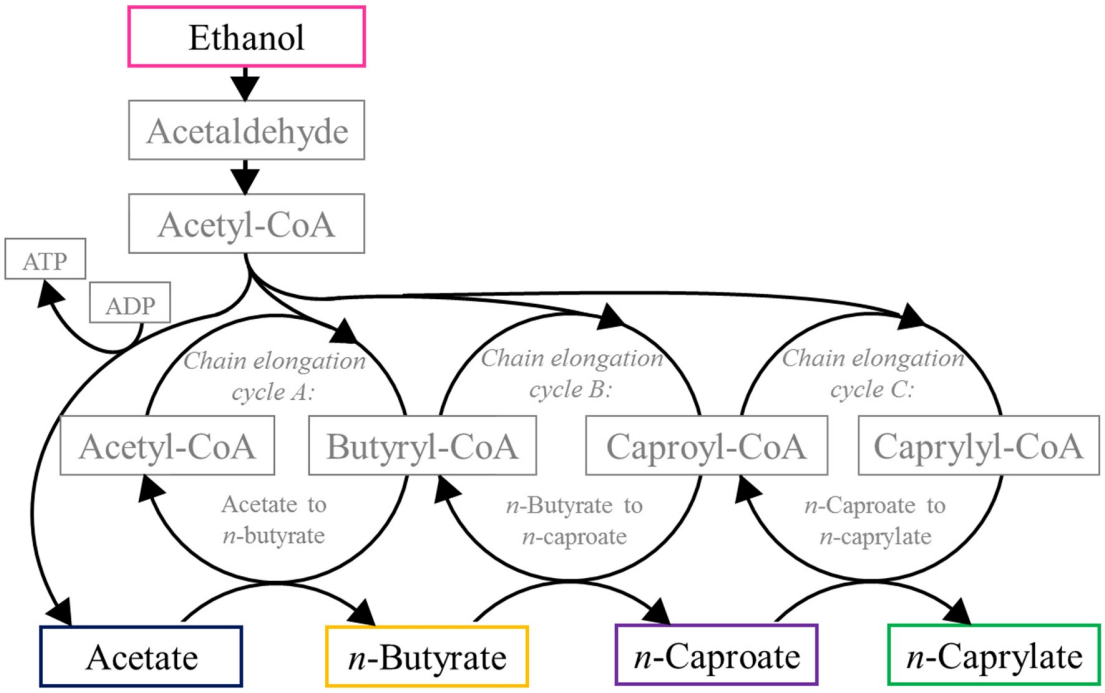

Figure S1: The reverse β-oxidation pathway. With the addition of ethanol, short-chain carboxylates (*e.g.* acetate) can be chain elongated to medium-chain carboxylates (*e.g. n*-caprylate). Based on Spirito et al. [1].

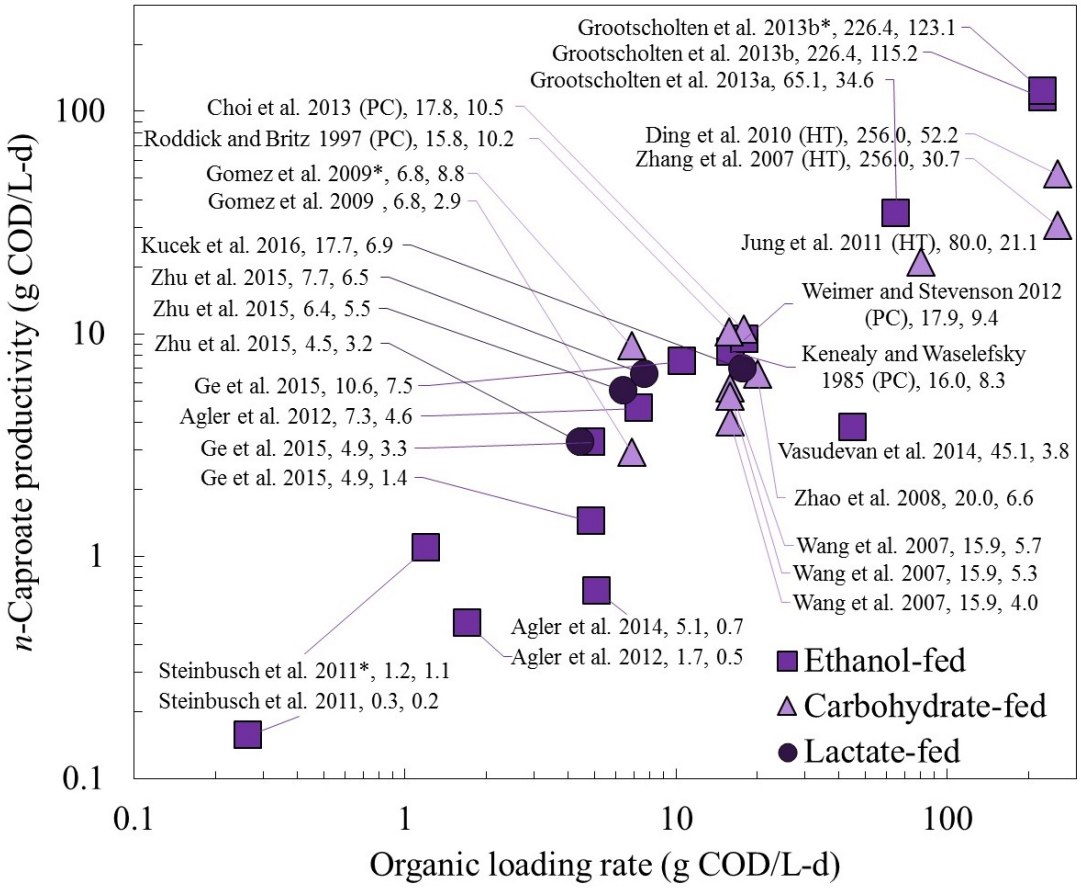

Figure S2: *n*-Caproate productivities. Results from 19 studies with high MCC production performances (*e.g.* concentrations, productivity). Indications include: methanogen-suppression *via* heat treatment (HT) with microbiomes; use of pure cultures (PC), such as *Megasphaera elsdenii* and *Clostridium kluyveri*; and maximum instantaneous values reported (*). The referenced study (see main text), the organic loading rate (OLR), and the *n*-caproate productivity are listed for each data point. Both *n*-caproate productivity and OLRs are presented on logarithmic scales.

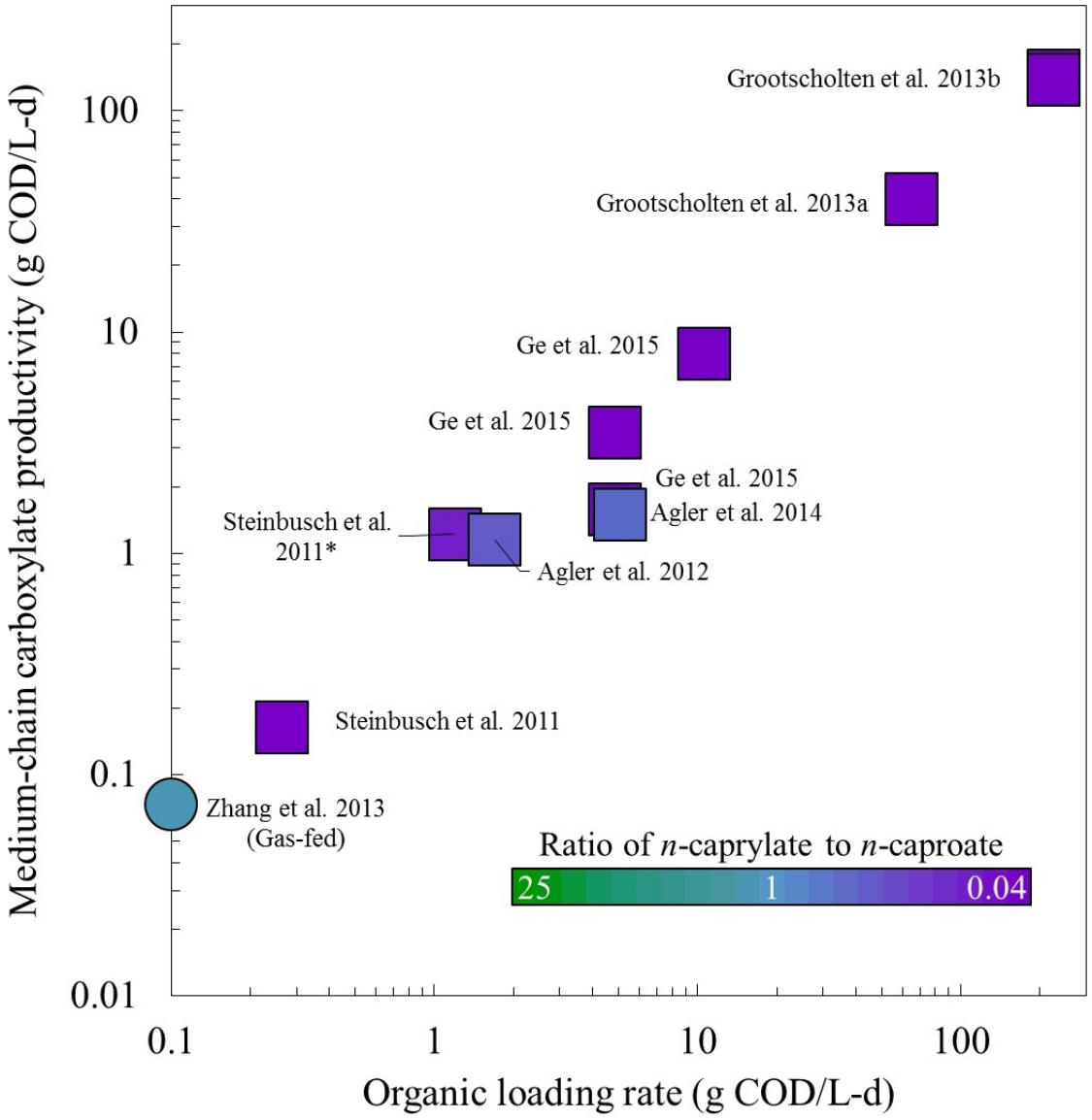

Figure S3: MCC productivity and product ratios of *n*-caprylate to *n*-caproate from bioreactors with ethanol as an electron donor. Results are from seven studies in which *n*-caprylate and *n*-caproate production were reported with ethanol in the substrate solution (squares); or with a gaseous substrate consisting of carbon dioxide and hydrogen (circle). For this gaseous substrate, ethanol was likely formed first as an intermediate, which is explained in the main text. Maximum instantaneous values reported are indicated (*). Both MCC productivities and organic loading rates (OLRs) are presented on logarithmic scales. Zhang et al. [2] did not report OLRs, so the circle was placed at an OLR near the sum of the total carboxylate volumetric production rates. A color gradient was used to show the product ratio of *n*-caprylate (green) to *n*-caproate (purple) with blue representing a more equal mixture of these two products. Product ratios of *n*-caprylate to *n*-caproate were: 0.04 [3]; 0.05 [4]; 0.06 [5]; 0.12* [6]; 0.50 [7]; 0.57 [8]; and 1.47 [2].

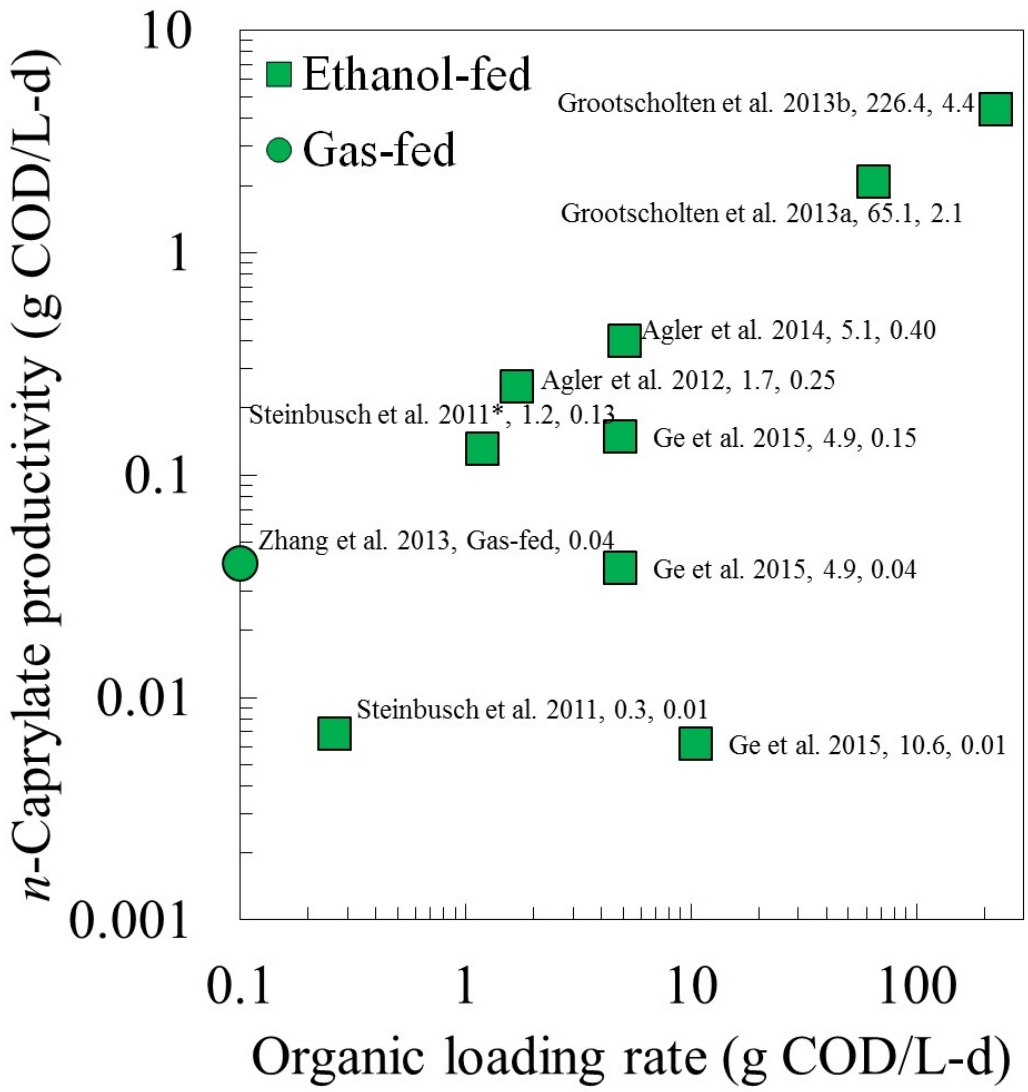

Figure S4: *n*-Caprylate productivities from bioreactors with ethanol as an electron donor. Results from seven previously published studies in which *n*-caprylate production was reported (squares and a circle). Maximum instantaneous values reported are indicated (*). The referenced study (see main text), the organic loading rate (OLR), and the *n*-caprylate productivity are listed. Both *n*-caprylate productivities and OLRs are presented on logarithmic scales. Zhang et al. [2] produced *n*-caprylate in a bioreactor in which gas composed of carbon dioxide and hydrogen was fed (see main text); they did not report OLRs, so this marker was placed at an OLR near the sum of the total carboxylate volumetric production rates.

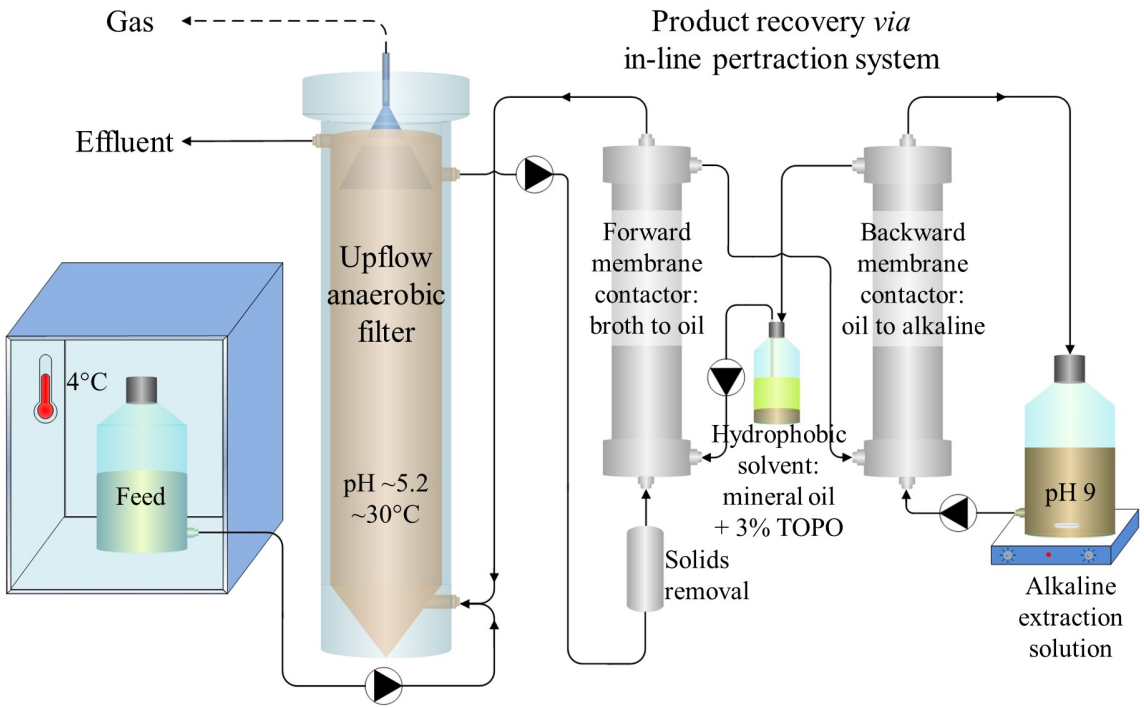

Figure S5: **Bioreactor system schematic**. An upflow anaerobic filter was continuously fed with a synthetic medium, which contained ethanol and acetate. In-line product extraction *via* pertraction (membrane-based liquid-liquid extraction) was used to continuously recover hydrophobic, undissociated medium-chain carboxylic acids (MCCAs) from a bioreactor broth recycle flow through the forward membrane contactor. After intermediary recovery in a mineral oil solvent, MCCAs were then transferred across a second, backward membrane contactor to an alkaline extraction solution. Through automatic base addition to the alkaline extraction solution, the pH gradient was maintained, and these products accumulated in the alkaline extraction solution as medium-chain carboxylates (MCCs). Adapted from Kucek et al. [9].

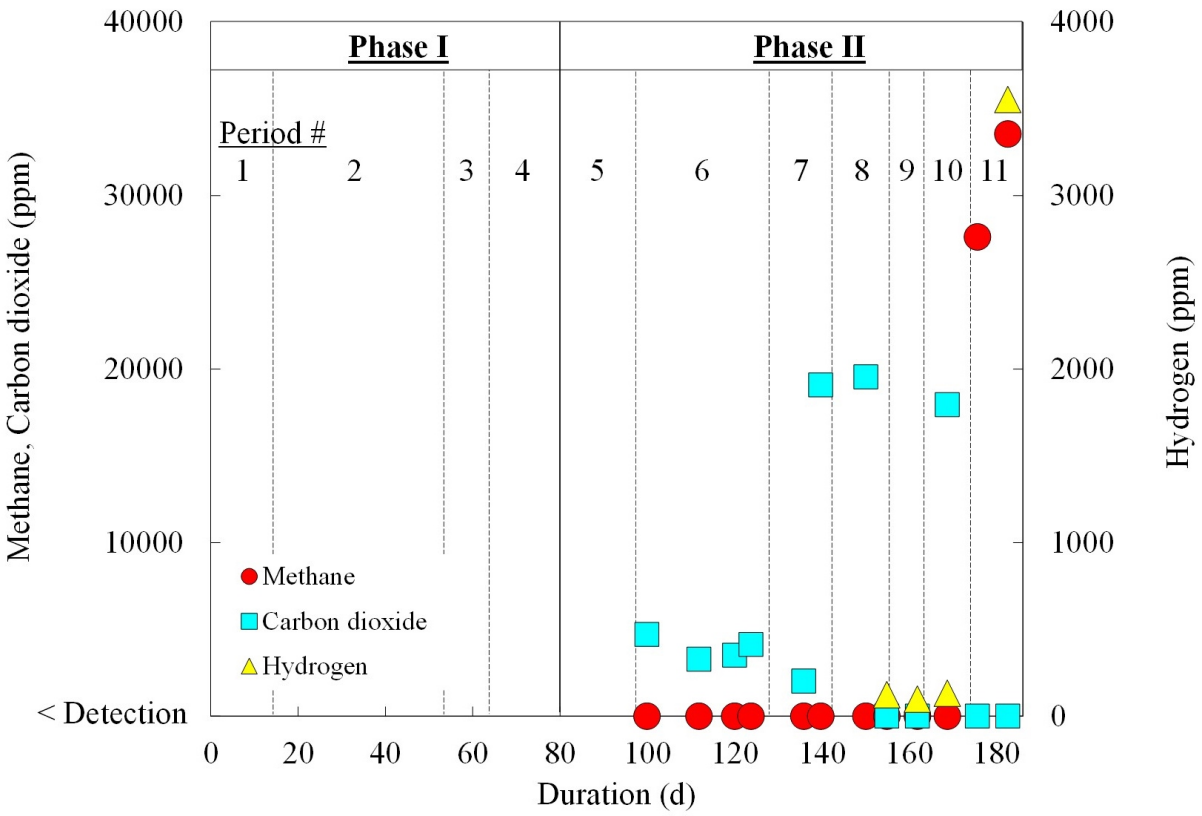

Figure S6: Biogas composition during Phase II. Hydrogen was quantified using the reduced gas detector at concentrations beneath 2000 ppm, while it was quantified with a gas chromatograph at higher concentrations. Methane concentrations were undetectable until Period 11 in Phase II, and the methane increase corresponded with increasing hydrogen concentrations and undetectable carbon dioxide concentrations.

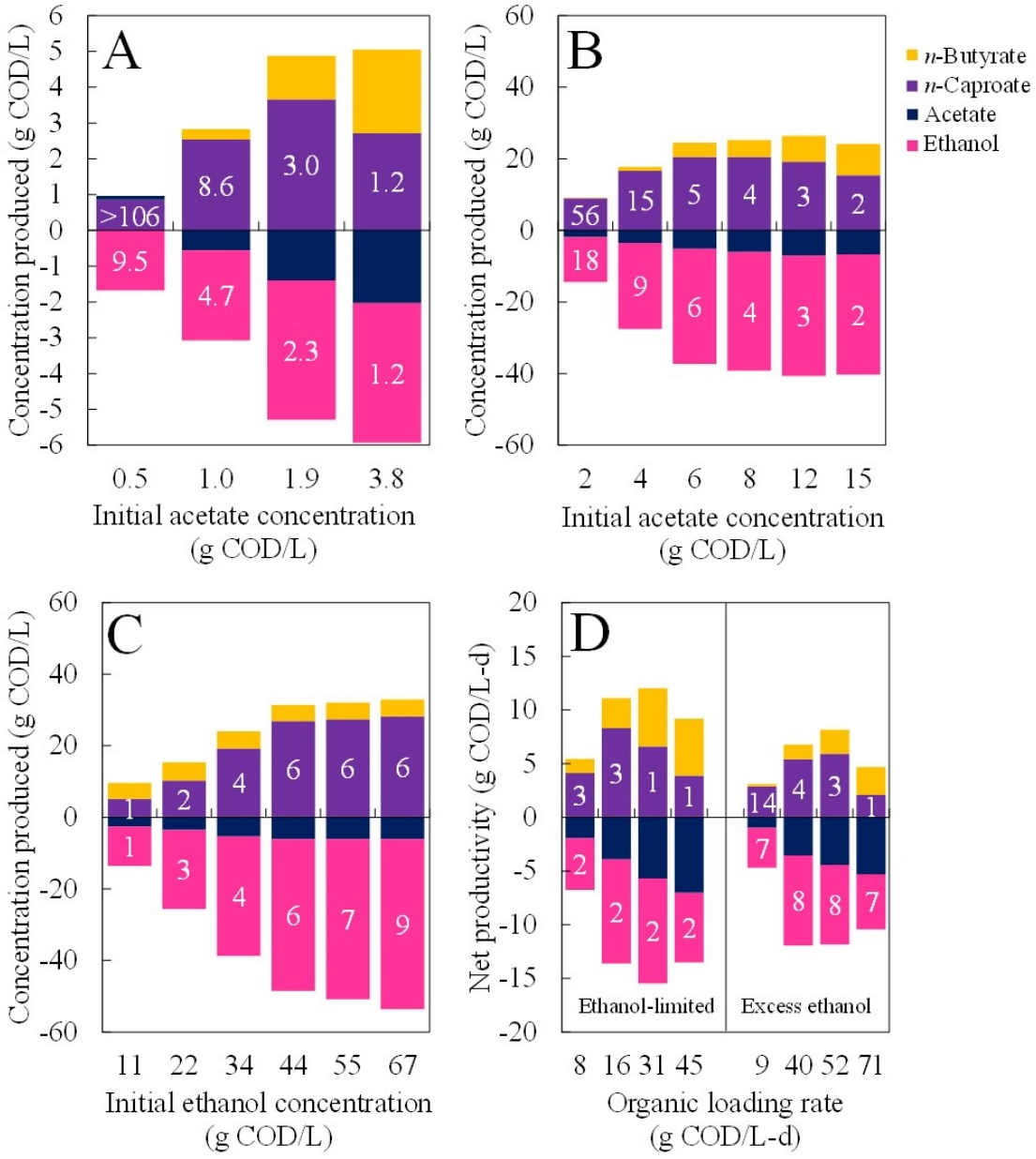

Figure S7: In previous studies, substrate ratios and concentrations affected carboxylate product ratios and concentrations in batch and continuously fed bioreactors of *C. kluyveri*. For (A)-(C), the concentrations of ethanol and carboxylates that were either produced (positive values) or consumed (negative values) are shown for batch bioreactor experiments of *C. kluyveri*. For (D), the net volumetric production rate (productivity) of ethanol and carboxylates that were either produced (positive values) or consumed (negative values) are shown for a continuously fed bioreactor of *C. kluyveri*. In all experiments, ethanol and acetate were fed. The initial substrate ratio (ethanol to acetate) for each treatment is displayed in white font upon the concentration of the ethanol consumed. In addition, the product ratio (*n*-caproate to *n*-butyrate) for each treatment is displayed in white font upon the concentration of the *n*-caproate produced. More specifically: (A) From Bornstein and Barker [10]: in this batch study, the initial concentration of ethanol was fixed (4.5 g COD/L, 47 mM) and the initial concentration of acetate was varied. The bioreactor temperature was 30°C, the pH was 7, and the duration was 12 d. When the initial concentration of acetate was increased, the ratio of *n*-caproate to *n*-butyrate produced decreased. At the

maximum initial concentration of acetate fed, the produced *n*-caproate concentration decreased; (B) From Weimer and Stevenson [11]: in this batch study, the initial concentration of ethanol was fixed (33.6 g COD/L, 350 mM) and the initial concentration of acetate was varied. The bioreactor temperature was 39°C, the initial pH was 6.8, and the duration was 3 d. When the initial concentration of acetate was increased, the ratio of *n*-caproate to *n*-butyrate produced decreased. At the maximum initial concentration of acetate fed, the produced *n*-caproate concentration decreased; (C) From Weimer and Stevenson [11]: in this batch study, the initial concentration of acetate was fixed (7.7 g COD/L, 120 mM) and the initial concentration of ethanol was varied. The bioreactor temperature was 39°C, the initial pH was 6.8, and the duration was 3 d. When the initial concentration of ethanol was increased, the ratio of *n*-caproate to *n*-butyrate produced increased until the initial concentration of ethanol was 44 g COD/L (460 mM); higher initial levels of ethanol led to substrate inhibition and decreased ethanol utilization; and (D) From Kenealy and Waselefsky [12]: in this continuously fed bioreactor study, the substrate ratio of ethanol to acetate was either ethanol-limited or had excess ethanol (2 or ~7 g COD/g COD, respectively). Increased substrate ratios and decreased substrate concentrations led to increased product ratios.

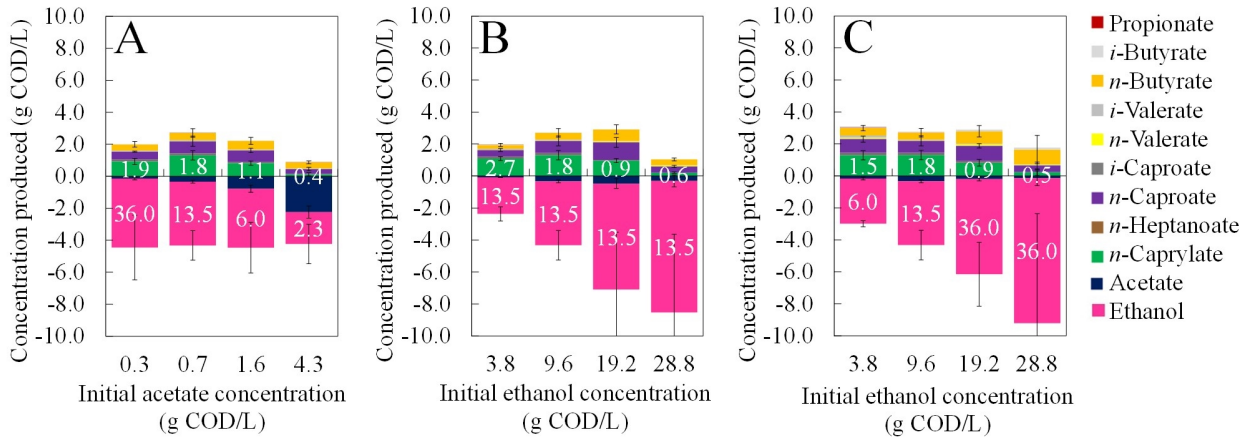

Figure S8: Substrate ratios and ethanol concentrations affected MCC product ratios and concentrations in batch reactor microbiomes. The concentrations of carboxylates that were produced (positive values) and the ethanol and acetate that were consumed (negative values) are shown for three batch experiments with reactor microbiomes, which we performed. In all experiments, ethanol and acetate were fed, and each concentration represents the average of triplicate biological batch bottles. The temperature of the bioreactors was controlled at 30°C and the initial pH was set at approximately 5.4 with an experimental period of 12 d. The initial substrate ratio (ethanol to acetate) for each treatment is displayed in white font within the pink bar for the ethanol concentration consumed, while the product ratio (*n*-caprylate to *n*-caproate) for each treatment is displayed in white font in the center of the green bar for the *n*-caprylate concentration produced. More specifically: (A) the initial concentration of ethanol was fixed (9.6 g COD/L, 100 mM) and the initial concentration of acetate was varied. When the initial concentration of acetate was increased (which consequently decreased the initial substrate ratio of ethanol to acetate), the product ratios of *n*-caprylate to *n*-caproate decreased. Increased substrate ratios of ethanol to acetate led to increased *n*-caprylate product ratios; (B) the initial substrate ratio of ethanol to acetate was fixed (13.5 g COD/g COD) and the substrate levels were varied. At this fixed substrate ratio, the lower substrate concentrations resulted in the higher product ratios of *n*-caprylate to *n*-caproate, as well as the higher concentrations of *n*-caprylate. At initial ethanol concentrations of 28.8 g COD/L (300 mM), considerable substrate inhibition of MCC production was observed; and (C) the initial acetate concentration was fixed (~0.7 g COD/L, ~10 mM) and the initial concentrations of ethanol were varied. An initial concentration of ethanol of 28.8 g COD/L (300 mM) led to substrate inhibition of chain elongation, even with fixed acetate concentrations. Error bars represent the standard error.

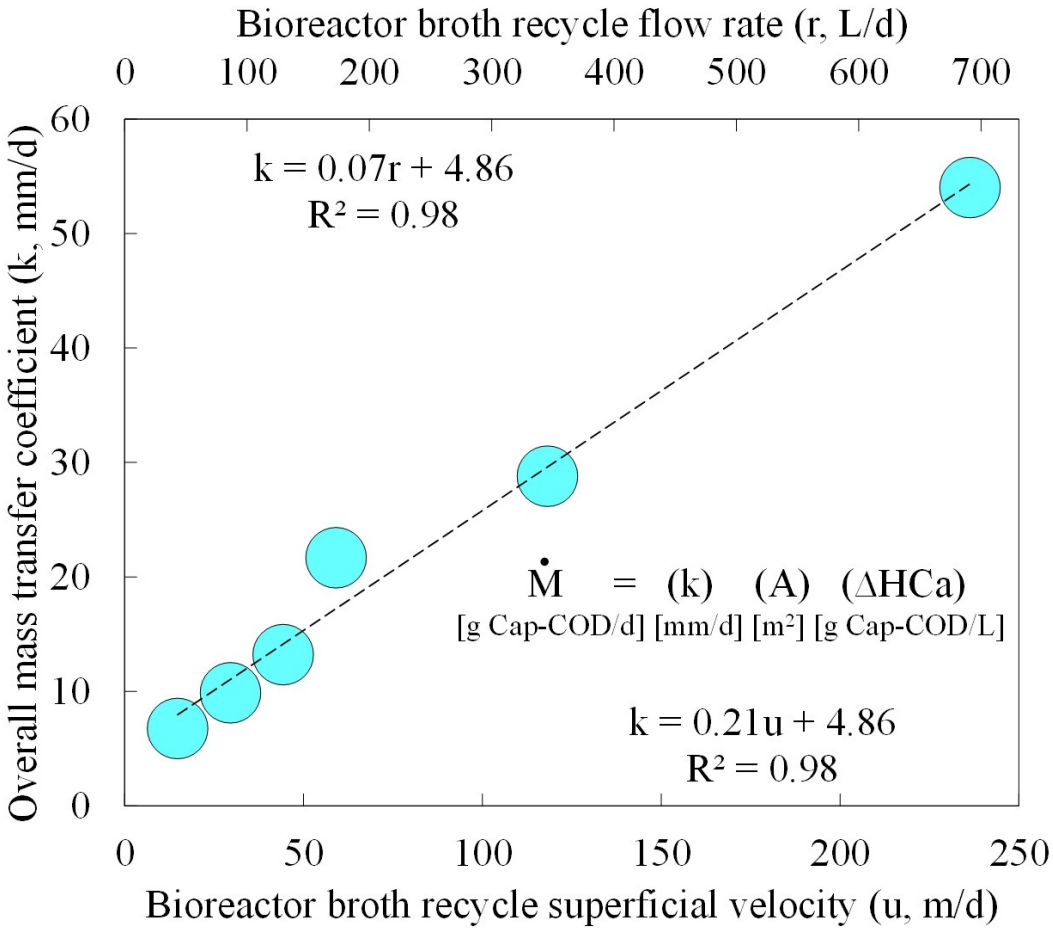

Figure S9: The overall mass transfer coefficient was directly proportional to the abiotic reactor broth recycle flow rate. During an abiotic *n*-caproic acid transfer experiment, we operated a pertraction system similar to the one we used in the bioreactor experiment (same materials, but a different size of contactors). We determined that the overall mass transfer coefficient (k) was directly proportional to the reactor broth recycle flow rate (r). The mass transfer coefficient in contactors of different sizes can be compared by correcting for the bioreactor broth recycle superficial velocity (u). Increasing the recycle flow rates of mineral oil solvent or the alkaline extraction solution did not affect the overall mass transfer rates, indicating that mass transfer limitations were at the interface of the reactor broth and the hydrophobic membrane contactor. The overall mass transfer coefficient was linearly correlated to the reactor broth recycle flow rate through the highest flow rates that the pumps could provide (690 L/d). During the continuously fed bioreactor experiment, however, we maintained a constant recycle flow rate (r, 130 L/d), mass transfer coefficient (k), and membrane surface area (A). With these fixed values fixed, improvements in MCC transfer (M) and production rates could only be achieved by higher concentrations of undissociated medium-chain carboxylic acids (MCCAs) in the bioreactor broth. The data here shows that we could have increased the MCC transfer rates with the same membrane contactors if we had increased the bioreactor broth recycle flow.

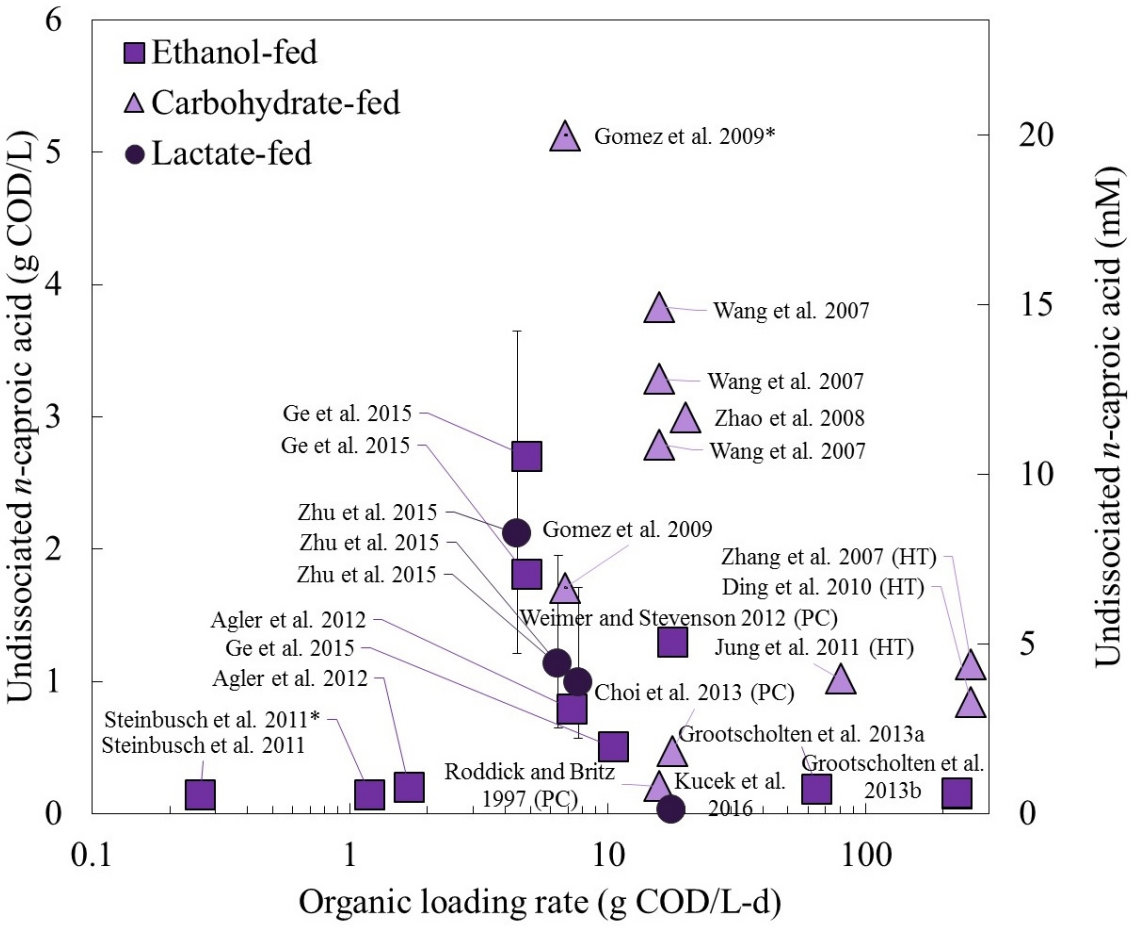

Figure S10: Bioreactor broth concentrations of undissociated *n*-caproic acid. Results from 16 published studies with high MCC productivities are shown. Uncertainty for the values from Zhu et al. [13] is based on the wide range of bioreactor pH values reported (pH 6.0-6.5). Indications include: 1) methanogen-suppression *via* heat treatment (HT); 2) use of pure cultures (PC) (*M. elsdenii* or *C. kluyveri*); and 3) maximum instantaneous values reported (*). Organic loading rates are presented on a logarithmic scale. Uncertainty is represented by 95% confidence intervals.

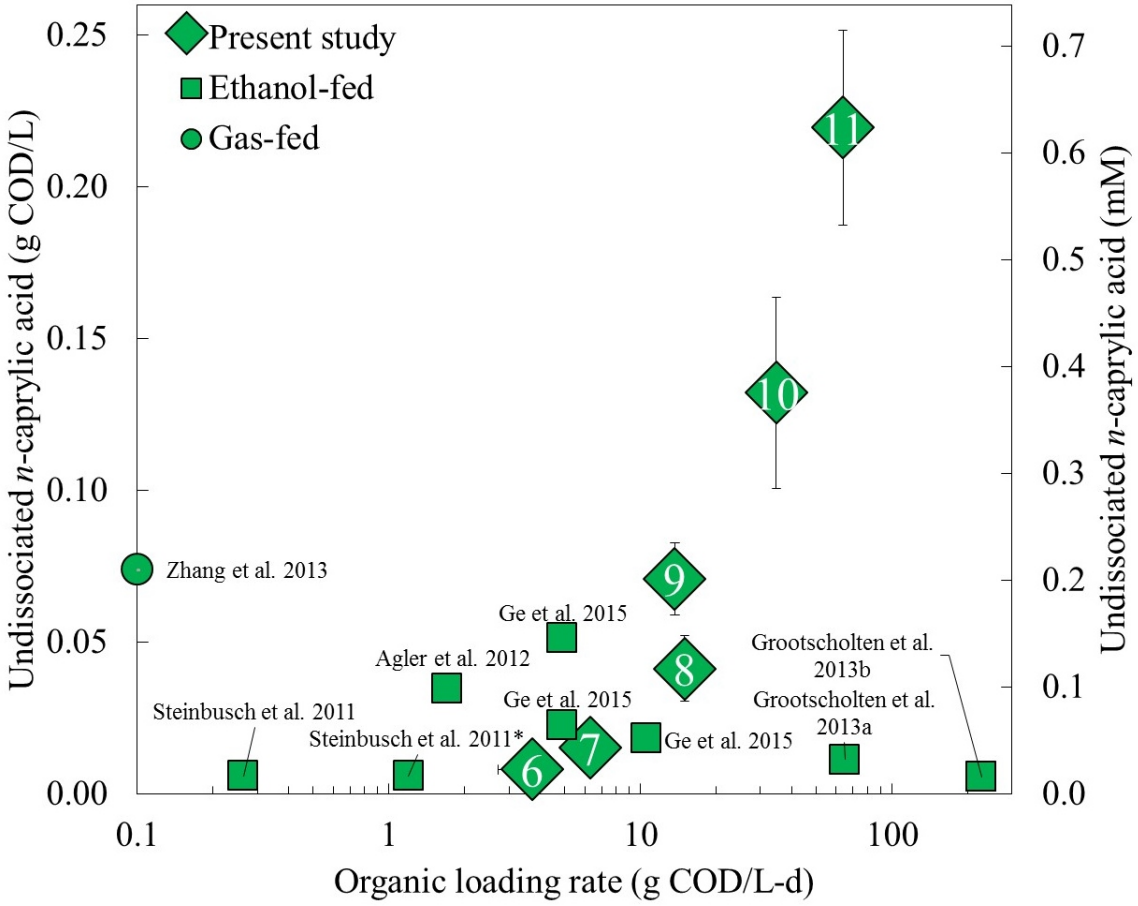

Figure S11: Undissociated *n*-caprylic acid concentrations from bioreactors with ethanol as an electron donor, including Phase II of this study. Results from seven studies in which *n*-caprylate production was reported are shown, including this study (large diamonds). Operating periods from Phase II of this study are labeled in white font. Maximum instantaneous values reported are indicated (*). Organic loading rates are presented on logarithmic scales. One study by Zhang et al. [2] produced *n*-caprylate in a bioreactor in which gas composed of carbon dioxide and hydrogen was fed (see text about ethanol as an intermediate); they did not report OLRs, so this marker was placed at an OLR near the sum of the total carboxylate volumetric production rates. The highest concentration of undissociated *n*-caprylic acid concentrations during Period 11 of our study likely led to product inhibition. Uncertainty is represented by 95% confidence intervals.

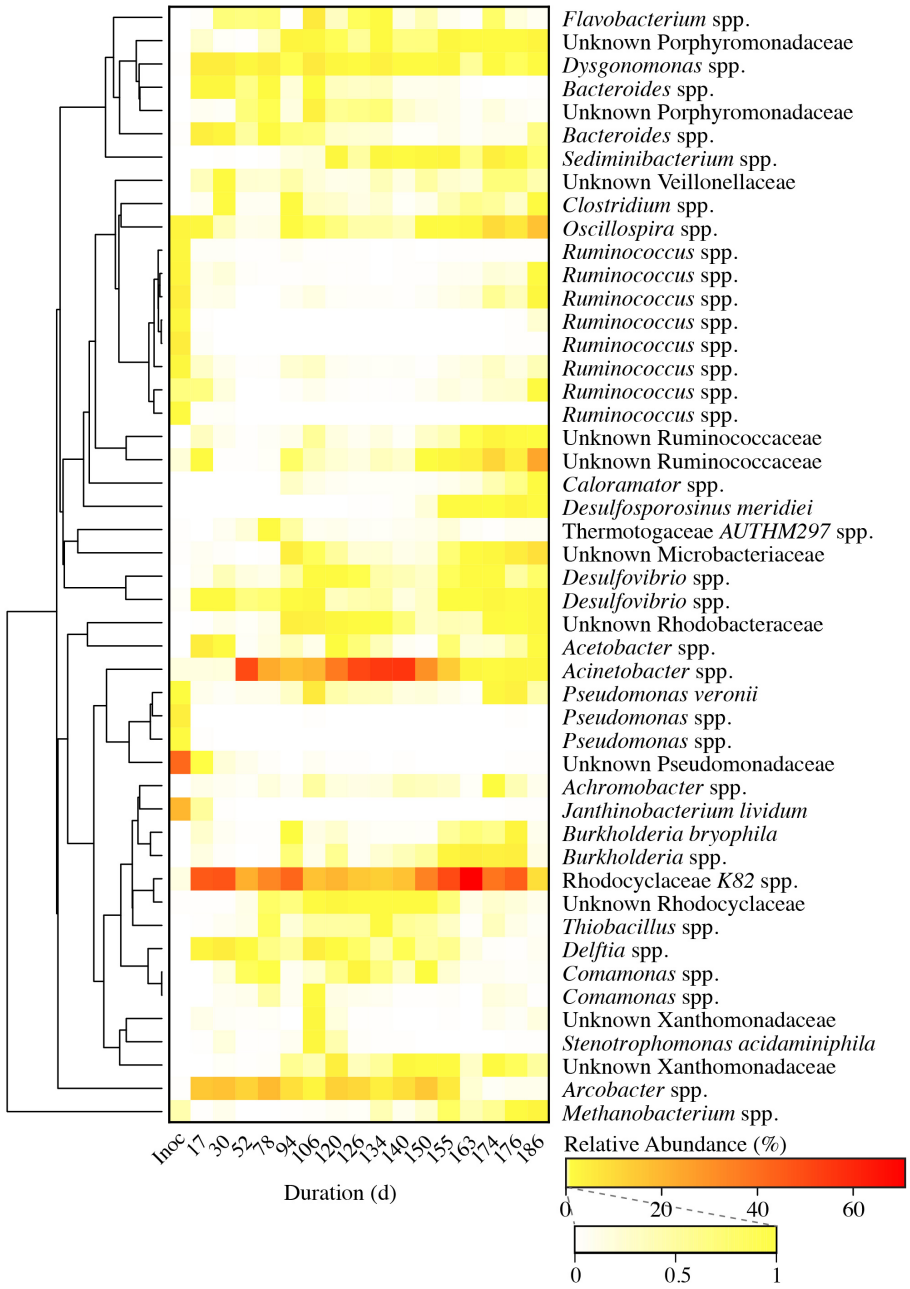

Figure S12: 48 OTUs with a relative abundance that exceeded 1% of at least one microbiome sample during the entire operating period. Relative abundances of operational taxonomic units (OTUs) varied during the operating period. Dominant OTUs included Rhodocyclaceae *K82* spp. and *Acinetobacter* spp., which comprised up to 70.8 and 55.5% of the relative abundance, respectively. Phylogenetic similarity is indicated.

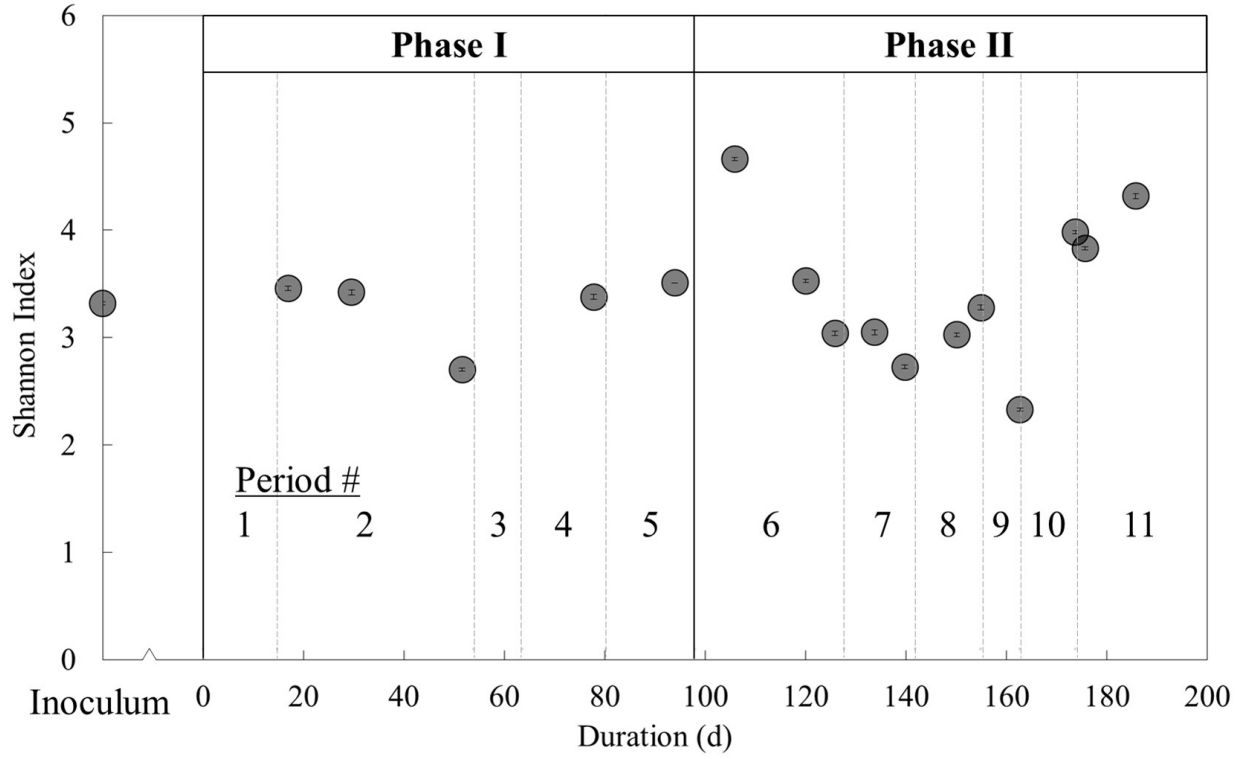

Figure S13: Alpha diversity of reactor microbiome sample during the entire operating period. The Shannon index was used to determine the evenness and richness for the 17 reactor microbiome samples that we collected, including the inoculum. Uncertainty is represented by 95% confidence intervals based on ten independent rarefactions.

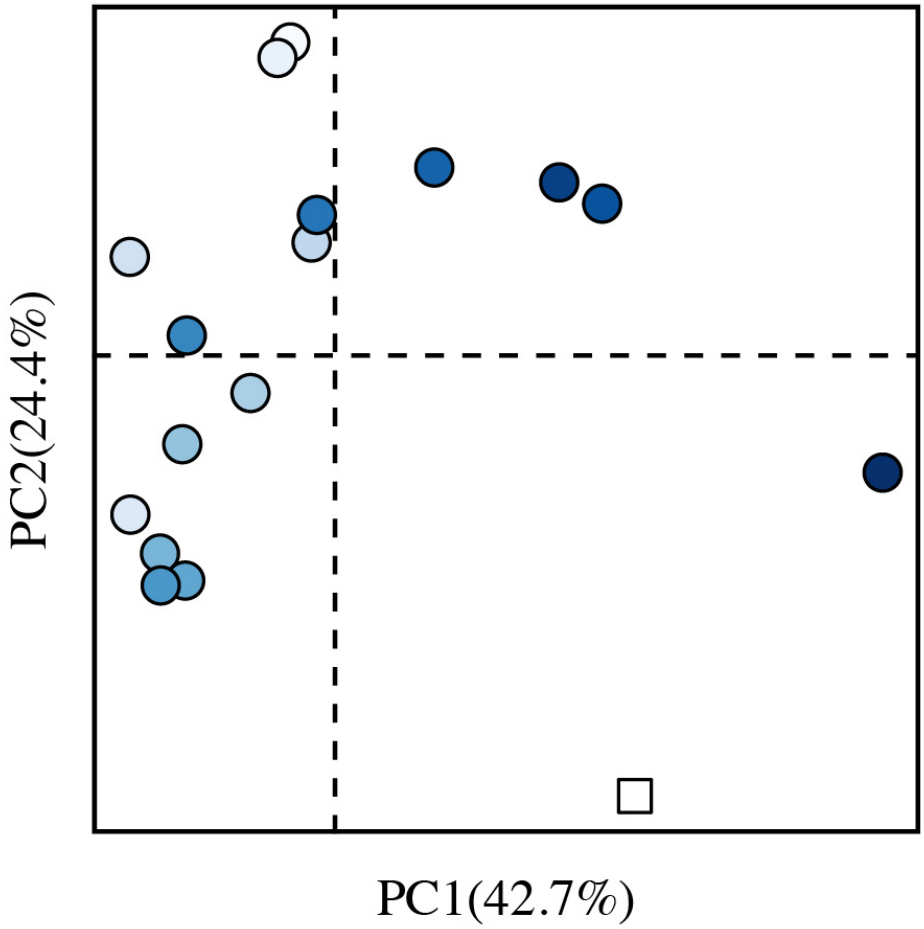

Figure S14: Beta diversity of the reactor microbiome samples during the entire operating period. Principal coordinates analysis (PCoA) was used to determine the dissimilarity between microbiome samples taken based on the weighted UniFrac metric. The first two principal coordinate (PC) axes are shown. PC1 explains 43% of the overall phylogenetic variation, while PC2 explains 24%. The increasingly darker blue color of the circles for the 16 bioreactor samples indicates the increasing length for the operating period when the sample was collected, including Day 17, 30, 52, 78, 94, 106, 120, 126, 134, 140, 150, 155, 163, 174, 176, and 186. The white square represents the inoculum.

Table S1: **Operating conditions and average bioreactor broth concentrations**. Average substrate and product concentrations in the bioreactor broth are reported for each operating period with their corresponding operating conditions. Detection limits were approximately 0.05 g COD/L (0.5 mM) for ethanol and approximately 0.02 g COD/L (~0.1 mM) for other carboxylates. B.D.: below detection. Uncertainty is represented by 95% confidence intervals.

Operating conditions					**Average bioreactor broth concentrations**					
Phase #	Period #	Pertraction +/-	Start - End *d*	Bioreactor pH	[Ethanol]	[*n*-Caprylate]	[*n*-Caproate]	[*n*-Butyrate]	[Acetate]	[Other SCC]
					g COD/L					
I	1	+	0 - 15	5.8 ± 0.6	1.01 ± 1.11	B.D.	0.80 ± 0.50	0.13 ± 0.08	0.64 ± 0.12	0.03 ± 0.03
	2	+	15 - 54	5.6 ± 0.2	0.10 ± 0.01	B.D.	0.19 ± 0.07	0.11 ± 0.05	0.57 ± 0.09	0.02 ± 0.01
	3	+	54 - 64	5.4 ± 0.1	0.10 ± 0.01	0.05 ± 0.12	0.03 ± 0.09	0.01 ± 0.01	0.39 ± 0.10	0.01 ± 0.03
	4	-	64 - 80	5.5 ± 0.1	0.04 ± 0.04	0.21 ± 0.14	0.23 ± 0.12	0.03 ± 0.03	0.61 ± 0.08	0.05 ± 0.03
	5	-	80 - 98	5.3 ± 0.1	0.25 ± 0.24	0.76 ± 0.16	1.03 ± 0.33	0.60 ± 0.24	0.75 ± 0.10	0.15 ± 0.03
II	6	+	98 - 128	5.2 ± 0.1	0.03 ± 0.05	0.03 ± 0.02	0.07 ± 0.02	0.08 ± 0.02	0.22 ± 0.05	0.01 ± 0.01
	7	+	128 - 142	5.1 ± 0.1	0.02 ± 0.05	0.04 ± 0.02	0.09 ± 0.02	0.07 ± 0.02	0.13 ± 0.06	0.03 ± 0.02
	8	+	142 - 155	5.0 ± 0.1	0.99 ± 0.20	0.09 ± 0.02	0.06 ± 0.04	0.00 ± 0.00	0.01 ± 0.02	0.06 ± 0.03
	9	+	155 - 163	5.1 ± 0.1	0.49 ± 0.24	0.18 ± 0.03	0.08 ± 0.03	0.05 ± 0.05	0.09 ± 0.04	0.05 ± 0.03
	10	+	163 - 174	5.1 ± 0.1	8.67 ± 2.12	0.34 ± 0.08	0.28 ± 0.06	0.11 ± 0.03	0.13 ± 0.02	0.09 ± 0.06
	11	+	174 - 186	5.2 ± 0.1	27.33 ± 3.01	0.69 ± 0.10	1.21 ± 0.11	1.09 ± 0.38	0.57 ± 0.12	0.04 ± 0.02

Table S2: **Operating conditions and average loading rates and carboxylate productivities.** Average productivities of medium-chain carboxylates (MCCs) (*e.g. n*-caprylate, *n*-caproate) and short-chain carboxylates (SCCs) are reported for each operating period with their corresponding operating conditions. These total productivities were calculated as the sum of average bioreactor effluent production rates plus average transfer rates *via* pertraction for each operating period, normalized to the bioreactor working volume. Acetate was continuously fed to the bioreactor, so negative production rates indicate net consumption of acetate. Uncertainty is represented by 95% confidence intervals. Total organic loading rates (OLRs) include loading from ethanol, acetate, and yeast extract. For most of the experiment, to vary the ethanol and total organic loading rates, the concentrations of ethanol and acetate in the basal medium were changed (instead of the HRT). The substrate ratio of ethanol to acetate was approximately 6 g COD/g COD until it was increased to 15 g COD/g COD on Day 80 of Phase I, Period 5. For each operating period, the concentrations of ethanol and total organics (g COD/L) in the continuously fed basal medium can be calculated by multiplying the reported average ethanol and total organic loading rates (g COD/L-d) by the corresponding average HRT (d). The yeast extract concentration in the media was consistently 1.6 g COD/L (1.25 g/L), and the corresponding yeast extract loading rate was approximately 0.4±0.1 g COD/L-d throughout the first 8 operating periods (HRT = 3.9±0.1 d). In Period 9, the feed flow rate was increased, which decreased the HRT, and the yeast extract loading rate was consequently increased to 1.1±0.1 g COD/L-d (HRT = 1.5±0.1 d). No considerable changes were observed in the *n*-caprylate or the total MCC productivities between Period 8 and Period 9. Uncertainty is represented by 95% confidence intervals.

Operating conditions				**Loading rates**		**Average carboxylate productvities**				
Phase	Period	Pertraction	HRT	Total OLR	Ethanol	*n*-Caprylate	*n*-Caproate	*n*-Butyrate	Net Acetate	Other SCC
#	#	+ / -	*d*	*g COD/L-d*		*g COD/L-d*				
I	1	+	4.2 ± 0.6	2.1 ± 0.6	1.4 ± 0.4	0.0 ± 0.0	0.5 ± 0.3	0.0 ± 0.0	-0.1 ± 0.1	0.0 ± 0.0
	2	+	4.8 ± 0.6	1.8 ± 0.1	1.2 ± 0.1	0.0 ± 0.0	0.3 ± 0.1	0.3 ± 0.2	-0.1 ± 0.0	0.3 ± 0.1
	3	+	3.8 ± 0.3	1.7 ± 0.4	1.2 ± 0.2	0.0 ± 0.0	0.6 ± 0.3	0.0 ± 0.0	-0.1 ± 0.0	0.0 ± 0.0
	4	-	4.5 ± 0.9	1.8 ± 0.3	1.2 ± 0.2	0.0 ± 0.0	0.1 ± 0.0	0.0 ± 0.0	-0.1 ± 0.0	0.0 ± 0.0
	5	-	4.4 ± 0.2	3.8 ± 0.4	3.2 ± 0.3	0.2 ± 0.0	0.2 ± 0.1	0.1 ± 0.1	0.0 ± 0.0	0.0 ± 0.0
II	6	+	3.7 ± 0.2	3.7 ± 0.4	3.1 ± 0.3	0.8 ± 0.1	1.2 ± 0.2	0.3 ± 0.1	-0.2 ± 0.0	0.0 ± 0.0
	7	+	3.8 ± 0.4	6.3 ± 0.4	5.6 ± 0.4	2.3 ± 0.4	2.2 ± 0.2	0.0 ± 0.0	-0.3 ± 0.0	0.1 ± 0.1
	8	+	3.3 ± 0.3	15.0 ± 2.9	13.7 ± 2.6	10.6 ± 0.3	0.4 ± 0.1	0.0 ± 0.0	-0.9 ± 0.2	0.0 ± 0.0
	9	+	1.6 ± 0.1	13.7 ± 1.8	12.2 ± 1.6	11.2 ± 1.5	1.7 ± 0.3	0.0 ± 0.0	-0.8 ± 0.1	0.3 ± 0.2
	10	+	1.5 ± 0.1	34.7 ± 2.7	31.8 ± 2.5	19.4 ± 1.1	1.7 ± 0.3	0.1 ± 0.0	-2.0 ± 0.2	0.1 ± 0.0
	11	+	1.5 ± 0.0	63.8 ± 6.7	59.1 ± 6.2	13.2 ± 0.8	7.5 ± 0.3	0.7 ± 0.2	-3.6 ± 0.4	0.0 ± 0.0

Table S3: **Operating conditions and average ethanol consumption, bioreactor performance, and pertraction efficiency.** Average bioreactor system performance for each of the operating periods are reported. Unconsumed ethanol rates were calculated by dividing the residual ethanol concentrations by the hydraulic retention times (HRTs). The percentage of ethanol consumed was calculated by dividing the ethanol consumption rate by the ethanol loading rate. The MCC conversion efficiency was calculated by dividing the MCC productivity by the total OLR. MCC product ratios represent the product ratio of *n*-caprylate to *n*-caproate. The pertraction efficiency was calculated for each MCCA by dividing the individual MCCA pertraction rate by the individual MCC production rate. The corresponding operating conditions are shown, including the bioreactor recycle broth rate of 130 L/d, which was the recirculation rate whether or not the pertraction system was in use. Uncertainty is represented by 95% confidence intervals.

Operating conditions				**Ethanol consumption**		**Conversion efficiency**	**MCC productivity**	**MCC ratio**	**Pertraction efficiency**	
Phase	Period	Pertraction	Recycle rate	% Consumed	Unconsumed				*n*-Caprylate	*n*-Caproate
#	#	+ / -	*L/d*	*%*	*g COD/L-d*	*g MCC-COD / g OLR-COD*	*g COD/L-d*	*g C8-COD / g C6-COD*	*%*	*%*
I	1	+	130	84% ± 40%	0.2 ± 0.3	23% ± 16%	0.5 ± 0.3	0.0 ± 0.0	0% ± 0%	61% ± 39%
	2	+	130	98% ± 11%	0.0 ± 0.0	15% ± 7%	0.3 ± 0.1	0.0 ± 0.0	0% ± 0%	85% ± 35%
	3	+	130	98% ± 29%	0.0 ± 0.0	35% ± 18%	0.6 ± 0.3	0.0 ± 0.1	0% ± 0%	98% ± 48%
	4	-	130	99% ± 25%	0.0 ± 0.0	5% ± 2%	0.1 ± 0.0	0.9 ± 0.7	NA	NA
	5	-	130	98% ± 15%	0.1 ± 0.1	11% ± 2%	0.4 ± 0.1	0.7 ± 0.3	NA	NA
II	6	+	130	100% ± 14%	0.0 ± 0.0	54% ± 8%	2.0 ± 0.2	0.7 ± 0.1	99% ± 9%	99% ± 26%
	7	+	130	100% ± 10%	0.0 ± 0.0	71% ± 9%	4.5 ± 0.5	1.0 ± 0.2	100% ± 27%	99% ± 13%
	8	+	130	98% ± 27%	0.3 ± 0.1	73% ± 14%	11.0 ± 0.3	25.2 ± 7.3	100% ± 4%	95% ± 40%
	9	+	130	98% ± 18%	0.3 ± 0.2	94% ± 17%	12.9 ± 1.5	6.6 ± 1.4	99% ± 19%	97% ± 24%
	10	+	130	82% ± 11%	5.7 ± 1.4	61% ± 6%	21.1 ± 1.1	11.2 ± 1.9	99% ± 8%	90% ± 21%
	11	+	130	70% ± 13%	18.0 ± 2.0	32% ± 4%	20.7 ± 0.9	1.8 ± 0.1	97% ± 9%	89% ± 4%

References

1. C. M. Spirito, H. Richter, K. Rabaey, A. J. M. Stams and L. T. Angenent, *Current Opin. Biotechnol.*, 2014, **27**, 115-122.
2. F. Zhang, J. Ding, Y. Zhang, M. Chen, Z.-W. Ding, M. C. M. van Loosdrecht and R. J. Zeng, *Water Res.*, 2013, **47**, 6122-6129.
3. T. I. M. Grootscholten, K. J. J. Steinbusch, H. V. M. Hamelers and C. J. N. Buisman, *Bioresour. Technol.*, 2013, **136**, 735-738.
4. S. Ge, J. Usack, C. M. Spirito and L. T. Angenent, *Environ. Sci. Technol.*, 2015, **49**, 8012-8021.
5. T. I. M. Grootscholten, K. J. J. Steinbusch, H. V. M. Hamelers and C. J. N. Buisman, *Bioresour. Technol.*, 2013, **135**, 440-445.
6. K. J. Steinbusch, H. V. M. Hamelers, C. M. Plugge and C. J. N. Buisman, *Energy Environ. Sci.*, 2011, **4**, 216-224.
7. M. T. Agler, C. M. Spirito, J. G. Usack, J. J. Werner and L. T. Angenent, *Energy Environ. Sci.*, 2012, **5**, 8189-8192.
8. M. T. Agler, C. M. Spirito, J. G. Usack, J. J. Werner and L. T. Angenent, *Water Sci. Technol.*, 2014, **69**, 62-68.
9. L. A. Kucek, M. Nguyen and L. T. Angenent, *Water Res.*, 2016, **93**, 163-171.
10. B. T. Bornstein and H. A. Barker, *J. Biol. Chem.*, 1948, **172**, 659-669.
11. P. J. Weimer and D. M. Stevenson, *Appl. Microbiol. Biotechnol.*, 2012, **94**, 461-466.
12. W. R. Kenealy and D. M. Waselefsky, *Arch. Microbiol.*, 1985, **141**, 187-194.
13. X. Zhu, Y. Tao, C. Liang, X. Li, N. Wei, W. Zhang, Y. Zhou, Y. Yang and T. Bo, *Sci. Rep.*, 2015, **5**, 14360.